- 3 -
ACOUSTICS

WAVE MOTION IN A FLUID MEDIA

3.1 The Wave Equation[1]

The fundamental equation of acoustics is the Helmholtz Equation or the Wave Equation. This equation is a derivative of the much more general, but nonlinear Navier-Stokes equation for fluids. The Wave Equation can be derived from the Navier-Stokes equation by assuming that the medium is linear and retaining only first order terms linear in pressure. If the acoustic medium is linear then waves of different frequencies will not interact with one another, i.e. superposition holds. The assumption of linearity of the medium is generally accurate for audio acoustics, except in some specific circumstances, which will be discussed later. Assuming linearity in the transducer itself is not at all accurate, but fortunately for us we need only require the medium to be linear. The medium of air only deviates significantly from this linear assumption at sound pressure levels (SPL) of about $2.0\,\mathrm{Nt/m^2}$ or above 140 dB (SPL). This is a substantial sound level that is seldom encountered in a free field and, hopefully, never at the receiver – the ear. However, it can be encountered in small spaces within the transducer itself.

The Wave Equation can be substantially simplified by the use of complex notation. When a complex exponential is assumed for the time dependence

$$\Psi(t) = \Psi \cdot e^{i\omega t} \tag{3.1.1}$$

and we insert this form into the Wave Equation,

$$\Delta^2\Psi(t) - \frac{1}{c^2}\frac{\partial^2\Psi(t)}{\partial t^2} = 0 \tag{3.1.2}$$

we get a second order partial differential equation where Δ^2 is the Laplacian operator. The new equation, which is the simpler Helmholtz Equation

$$\Delta^2\Psi(\omega) - k^2\Psi(\omega) = 0 \tag{3.1.3}$$

$k = \omega/c$ *the wavenumber in* m^{-1}

$c =$ *the speed of sound in the medium in* ms^{-1}

---

1. See Morse, *Methods of Theoretical Physics, Vibration and Sound or Theoretical Acoustics*

Eq. (3.1.3) will form the basis of all our discussions in this chapter. For convenience we will usually drop any specific reference to either the time dependence t or the frequency dependence ω as they will be assumed. For linear solutions this is not a problem since an arbitrary solutions in frequency can be built up of a sum of solutions at a particular frequency, as we saw in Chap.1. Dropping these complex dependencies greatly simplifies the writing, although we must be careful to always remember their continuous presence.

The operator

$$\Delta^2\Psi = \frac{\partial^2\Psi}{\partial x^2} + \frac{\partial^2\Psi}{\partial y^2} + \frac{\partial^2\Psi}{\partial z^2} \tag{3.1.4}$$

is the Laplacian, shown here in the familiar Rectangular coordinate system. It is different in every coordinate system.

The Helmholtz Equation describes a scalar field in the scalar quantity Ψ, the velocity potential. It is called the velocity potential since the field velocity is its negative gradient. It has no physical significance but is a convenient quantity for us to use since either of the quantities of interest to us, pressure and particle velocity, can be derived from it directly.

The equations for the pressure p and the velocity v are

$$p = -i\omega\rho c\,\Psi\,\vec{v} = -\Delta\Psi \tag{3.1.5}$$

from which it follows that

$$i\omega\rho\vec{v} = -\Delta \cdot p \tag{3.1.6}$$

ρ = *the density of the medium in kg / m.*

The quantities c and ρ both vary with temperature, static pressure and humidity (among other things), but these variations are usually negligible. (Although we will see that in room acoustics these variations, however small, have a profound effect.)

The appearance of the Helmholtz Equation can be quite deceptive. Its solution in the general case would take an entire volume or more to thoroughly investigate. We will investigate numerous solutions of the Wave Equation, but in only a few different coordinate systems, and then with only a few specific boundary conditions.

3.2 The Helmholtz Equation in Rectangular Coordinates [2]

Solutions in Rectangular Coordinates are relatively easy compared to those in other coordinate systems. Unfortunately they are not a great deal of use to us in this text. Still, we can learn a significant amount about the general approach to the solution of the Helmholtz Equation in other coordinate systems by investigating the simpler solutions in Rectangular Coordinates.

---

2. See Morse, *Vibration and Sound* and *Methods of Theoretical Physics.*

In Rectangular Coordinates the Helmholtz Equation is

$$\frac{\partial^2\Psi}{\partial x^2}+\frac{\partial^2\Psi}{\partial y^2}+\frac{\partial^2\Psi}{\partial z^2}-k^2\Psi=0 \tag{3.2.7}$$

Let us assume a solution that is the product of three separate solutions:

$$\Psi(x,y,z)=X(x)Y(y)Z(z) \tag{3.2.8}$$

We will find that, in general, the solutions to almost any problem starts with an assumed solution which is then plugged back into the original equations in order to find out how well it fits. So assuming the general solution to be the product of three separate solutions in each of the three spatial coordinates is a reasonable place to start. Hindsight is also helpful.

Using Eq. (3.2.8) in Eq. (3.2.7) results in

$$\frac{1}{X(x)}\frac{\partial^2X(x)}{\partial x^2}+\frac{1}{Y(y)}\frac{\partial^2Y(y)}{\partial y^2}+\frac{1}{Z(z)}\frac{\partial^2Z(z)}{\partial z^2}+k^2=0 \tag{3.2.9}$$

which we can rewrite as

$$\frac{1}{X(x)}\frac{\partial^2X(x)}{\partial x^2}=k^2-\frac{1}{Y(y)}\frac{\partial^2Y(y)}{\partial y^2}-\frac{1}{Z(z)}\frac{\partial^2Z(z)}{\partial z^2} \tag{3.2.10}$$

by simply rearranging the terms.

For both sides of this equation to hold they must both be equal to a common constant. This last statement is a powerful argument, the validity of which is crucial to all of the following discussions. Its legitimacy is apparent by thinking about two functions, of different variables, varying independently, but yet still being equal. We will call this value the *separation constant*.

Setting both sides of Eq. (3.2.10) equal to the common constant k_x^2 we will obtain

$$\frac{1}{X(x)}\frac{\partial^2X(x)}{\partial x^2}=k^2-\frac{1}{Y(y)}\frac{\partial^2Y(y)}{\partial y^2}-\frac{1}{Z(z)}\frac{\partial^2Z(z)}{\partial z^2}=k_x^2 \tag{3.2.11}$$

from which it follows that

$$\begin{aligned}&\frac{1}{X(x)}\frac{\partial^2X(x)}{\partial x^2}=k_x^2 \quad \textit{and}\\ &\frac{1}{Y(y)}\frac{\partial^2Y(y)}{\partial y^2}+\frac{1}{Z(z)}\frac{\partial^2Z(z)}{\partial z^2}=k^2-k_x^2\end{aligned} \tag{3.2.12}$$

Following along with this same process, once again, we find a complete set of separated equations, each one conveniently in a single dependent variable, even though coupled together by a common constant. This set is

$$\frac{\partial^2 X(x)}{\partial x^2} - k_x^2 X(x) = 0$$
$$\frac{\partial^2 Y(y)}{\partial y^2} + k_y^2 Y(y) = 0 \qquad (3.2.13)$$
$$\frac{\partial^2 Z(z)}{\partial z^2} - k_z^2 Z(z) = 0$$

$$k^2 = k_x^2 + k_y^2 + k_z^2 .$$

The wavenumber k is now in a form that is quite instructive, namely that it is actually a vector with elements k_x, k_y, and k_z in the x, y and z directions, respectively. This wavenumber vector concept, which we will call k-space, will become handy to us in the future.

The three separated equations are, conveniently, all identical and they are known to have simple, well known solutions

$$X(x) = A_x e^{ik_x x} + B_x e^{-ik_x x}$$
$$Y(y) = A_y e^{ik_y y} + B_y e^{-ik_y y} \qquad (3.2.14)$$
$$Z(z) = A_z e^{ik_z z} + B_z e^{-ik_z z}$$

where, as we has stated, we have ignored the time factor. These equations are often written in the equivalent form of sines and cosines.

Another useful form of this solution is to write

$$\Psi(\vec{r},t) = Ae^{i\omega t - \vec{k}\cdot\vec{r}} + Be^{i\omega t + \vec{k}\cdot\vec{r}} \qquad (3.2.15)$$

where we have written all of the spatial coordinates simply as a vector r to the spatial point and the separation constants as a vector k in k-space. For Rectangular Coordinates this formulation and concept is hardly necessary, although instructive, for we can see that the general plane wave solution is made up of wave components in the three orthogonal directions of the coordinate system. This will hold true for any coordinate system which is orthogonal. In Rectangular Coordinates it is hardly useful, but for more complex coordinate systems it will become very useful.

An example of the utility of the k-space concept is in the study of the low frequency sound field of a small rectangular room which we will study in far greater detail in Chap.7. A sound wave propagating at a particular mode (l, m, n) travels in a direction of k, given by

$$\vec{k} = \frac{l\pi}{L_x}\cdot\hat{i} + \frac{m\pi}{L_y}\cdot\hat{j} + \frac{n\pi}{L_z}\cdot\hat{k} \qquad (3.2.16)$$

where the room has dimension L_x by L_y by L_z. This implies that a sound source which excites only a single mode in such a room does not radiate sound in all directions, nor does the sound wave propagate freely about the room. The sound

wave is constrained to move in precise fixed directions as given by the above equation. A loudspeaker exciting this mode would have propagating sound waves emitted only in the direction of k. There would be a small direct field from this source, but otherwise its directivity would be fixed in space by the vector k. The concept of source directivity, as we will come to know it, does not exist in small rooms at low frequencies.

3.3 Cylindrical Coordinates[3]

In Cylindrical Coordinates we will encounter some significant complications to our problem, namely, that the solutions are functions that are not as well known as simple complex exponentials or sines and cosines.

In the Cylindrical coordinate system the Helmholtz Equation is

$$\frac{1}{r}\frac{\partial}{\partial r}\left(r\frac{\partial \Psi}{\partial r}\right)+\frac{1}{r^2}\frac{\partial^2 \Psi}{\partial \varphi^2}+\frac{\partial^2 \Psi}{\partial z^2}-k^2\Psi=0 \tag{3.3.17}$$

Once again, we will assume that a solution exists which relies on only a single spatial variable

$$\Psi(r,\varphi,z)=R(r)\Phi(\varphi)Z(z) \tag{3.3.18}$$

Following along lines, identical to the previous example, leads us to three separated equations in the three spatial variables, r, θ and z

$$\begin{aligned} &r^2\frac{d^2R(r)}{dr^2}+r\frac{dR(r)}{dr}+\left(r^2k^2-k_\varphi^2\right)R(r)=0 \\ &\frac{d^2\Phi(\varphi)}{d\varphi^2}+k_\varphi^2\Phi(\varphi)=0 \\ &\frac{d^2Z(z)}{dz^2}+k_z^2Z(z)=0 \end{aligned} \tag{3.3.19}$$

We have already seen the solutions to the last two equations

$$\Phi(\varphi)=Ae^{ik_\varphi\varphi}+Be^{-ik_\varphi\varphi} \tag{3.3.20}$$

and

$$Z(z)=Ae^{ik_z z}+Be^{-ik_z z} \tag{3.3.21}$$

In Eq. (3.3.20) the separation constant k_φ is not arbitrary, owing to the fact that the solution in φ must be periodic. Therefore k_φ must be an integer, which we will call m.

The separation constant k_z remains completely arbitrary and can take on any value within limits. As we will see, the k-space concept as a continuum is most appropriate for this type of continuous wavenumber.

---

3. Morse, *Methods of Theoretical Physics*, and *Theoretical Acoustics*

Given the above restriction on the separation constants, the equation for $R(r)$ in Eq. (3.3.19) becomes

$$r^2 \frac{d^2R(r)}{dr^2} + r\frac{dR(r)}{dr} + \left(r^2k^2 - m^2\right)R(r) = 0 \tag{3.3.22}$$

This equation, known as Bessel's equation, and has been thoroughly studied[4]. By assuming a solution as a power series in kr and inserting it into this equation we would find that a convergent series would result. This series has come to be know as a *Bessel Function.*

The solutions to *Bessel's equation* are then

$$R(r) = A\,J_m(kr) \tag{3.3.23}$$

J_m = *are Bessel Functions of order m*

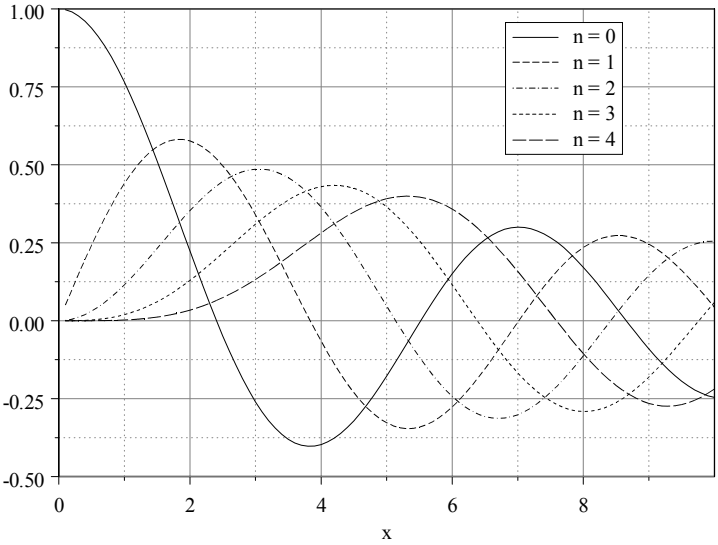

Figure 3-1 - Bessel Functions of order m

Each value of m exhibits a completely different function, but one which is orthogonal to all the other functions in m. The first five orders of this function are shown in Fig. 3-1 as a function of the argument kr (shown as x).

From Eq. (3.3.22) we can see that the equation is of second order in r and therefore must have a second solution, which must be orthogonal to the first. We can also see that the equation is singular at the origin, and as such, one of the solutions must also be singular at the origin. The Bessel Functions are not singular anywhere. The techniques for finding this second solution are generally known

4. See Morse, *Vibration and Sound.*

but these techniques are beyond the scope of this book. This second set of functions are known as Neumann functions and can be derived directly from the Bessel Functions. The singularity of these functions at the origin generally limits their usefulness to problems that do not contain the origin. Some of our problems are of this class, although many others are not. We must consider each case separately and decide if we must retain both solutions or not. Both of the solutions of Bessel's equation are a complete orthogonal set on the interval $r = \langle 0, \infty \rangle$ with a weighting function *kr*.

The complete solution to Eq. (3.3.22) thus becomes

$$R(r) = A \cdot J_m(kr) + B \cdot N_m(kr) \tag{3.3.24}$$

N_m = *are Neuman functions of order m.*

An alternative set of functions which we will have extensive use for are know as the Hankel Functions, and are denoted $H_m(kr)$. They are defined as

$$H_m^{(2)}(kr) = J_m(kr) - i\,N_m(kr) \tag{3.3.25}$$

The superscript 2 stands for "of the second kind" the first kind having a plus sign in the sum. One set represents outgoing waves and the other incoming waves. We will usually consider only outgoing waves and drop the superscript. These functions have the characteristics of a traveling wave in Cylindrical Coordinates, like the complex exponential functions in Rectangular Coordinates, the physical values being the real part.

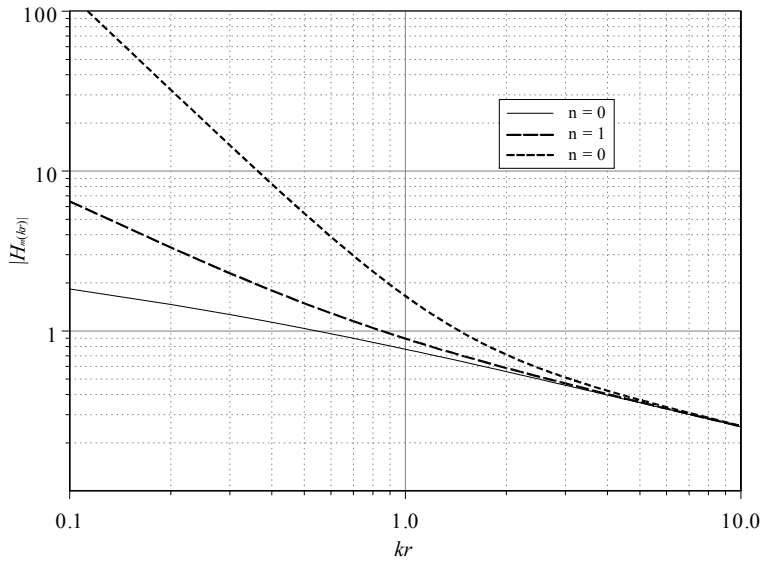

Figure 3-2 - Hankel Function magnitude for various orders

The magnitude of the Hankel Function waves is shown in Fig. 3-2. The real part of this function is identical to Fig. 3-1. The magnitudes of these waves all grow to infinity at the origin due to the presence of the Neumann functions. The higher the order of the function the faster they grow towards the origin, the singularity in the equation.

As we will see the Bessel Functions will be useful for problems that require standing wave solutions and the Hankel Functions for problems that have propagating solutions.

A useful fact is that the Bessel Functions are also orthogonal on a finite interval. An example is (one that we will have further use for shortly) when the problem dictates a two dimensional ($k_z = 0$) solution and a boundary condition is given for $R(r)$ at some finite radius $r = a$ – a circle. If the boundary condition is

$$\frac{\partial}{\partial r} R(a) = 0 \tag{3.3.26}$$

then the characteristic functions for this problem (those functions which satisfy the boundary conditions) are

$$\psi_n(r) = J_m\left(\beta_{0,n}\frac{r}{a}\right) \tag{3.3.27}$$

$\beta_{0,n}$ = *the characteristic (eigen) values*

such that

$$\frac{d}{dr} J_0(\beta_{0,n}\frac{r}{a})\bigg|_{r=a} = J_1(\beta_{0,n}) = 0 \tag{3.3.28}$$

The orthogonality integral for this set of Bessel Functions is

$$\int_0^{2\pi}\int_0^a \psi_{0,n}(r,\varphi)\psi_{0,n'}(r,\varphi)\, r\, dr\, d\varphi \begin{cases} 0 & n \neq n' \\ \pi a^2 J_1^{\,2}(\beta_{0,n}) & n = n' \end{cases} \tag{3.3.29}$$

This integral represents the normalization constants for the set of functions.

3.4 Spherical Coordinates[5]

In Spherical Coordinates, the solutions will bear a striking resemblance to those found in the cylindrical case. In this coordinate system the Helmholtz Equation is

$$\frac{1}{r^2}\frac{\partial}{\partial r}\left(r^2\frac{\partial \Psi}{\partial r}\right) + \frac{1}{r^2\sin(\theta)}\frac{\partial}{\partial \theta}\left(\sin(\theta)\frac{\partial \Psi}{\partial \theta}\right) + \frac{\partial^2 \Psi}{\partial \varphi^2} - k^2\Psi = 0 \tag{3.4.30}$$

5. See Morse, *Methods of Theoretical Physics*

Once again we will assume that a solution exists which relies on only a single spatial variable

$$\Psi(r,\theta,\varphi) = R(r)\Theta(\theta)\Phi(\phi) \tag{3.4.31}$$

Inserting this assumed solution into Eq. (3.4.30) yields the three separated equations

$$\begin{aligned} &r^2\frac{d^2R}{dr^2} + 2\ \ r\frac{dR}{dr} + \left(k^2r^2 - n(n+1)\right)R = 0 \\ &\sin\theta\frac{d}{d\theta}\left(\sin\theta\frac{d\Theta}{d\theta}\right) + \left[n(n+1)\sin^2\theta - m^2\right]\Theta = 0 \\ &\frac{d^2\Phi}{d\phi^2} + m^2\Phi = 0 \end{aligned} \tag{3.4.32}$$

The equation for $\Phi(\phi)$ is, by now, well known to us. We note that m must be an integer because of the periodic nature of the ϕ coordinate. For nearly all cases that we will encounter in this text m will be zero, i.e. there will be axi-symmetry about ϕ.

The equation for $R(r)$ looks new. However, with a simple change of variables this equation can be rewritten in a form whose solution we have already developed. By utilizing a new set of functions, which are based on Bessel Functions, we can obtain solutions to the radial equation. These new functions are obtained by multiplying the Bessel Functions by $kr^{-1/2}$ (and some other constants) and using new orders of $n+1/2$. These new functions satisfy Eq. (3.4.32) for $R(r)$. They are

$$\begin{aligned} R(r) &= \sqrt{\frac{\pi}{2kr}}\left(J_{n+\frac{1}{2}}(kr) - iN_{n+\frac{1}{2}}(kr)\right) \\ &= \sqrt{\frac{\pi}{2kr}}\cdot H^{(2)}_{n+\frac{1}{2}}(kr) \\ &= h^{(2)}_n(kr) \end{aligned} \tag{3.4.33}$$

where we have introduced a new symbol $h_n(kr)$ for these new functions. These functions are called the *Spherical Hankel Functions of the second kind of order* n. The spherical solutions are of sufficient importance that they have been allocated their own name, even though they are a simple derivative of the Bessel Functions. We will only be concerned with outgoing waves and so we will usually drop the superscript (2) which plays the same role here as it did for the cylindrical case. Numerical values and algorithms for these functions are readily available.[6,7]

The equation in θ is new to us and warrants some discussion. It is usually solved after transforming variables to $\mu = \cos(\theta)$ giving us an equation in μ:

---

6. see Morse and Ingard, *Theoretical Acoustics*
7. see Press, et. al. *Numerical Recipes*

$$(1-\mu^2)\frac{d^2T(\mu)}{d\mu^2} - 2\mu\frac{dT(\mu)}{d\mu} + \left[n(n+1) - \frac{m^2}{(1-\mu^2)}\right]T(\mu) = 0 \tag{3.4.34}$$

where we have written these new function as $T(\mu)$. Solutions of this equation turn out to be describable by a finite series in m with order n and degree m. They are called the *Associated Legendre Functions* $T_{nm}(\mu)$ where

$$T_{nm}(\mu) = (1-\mu^2)^{m/2}\frac{d^m P_n(\mu)}{d\mu^m} \tag{3.4.35}$$

$P_n(u)$ = *the Legendre Polynomials of order n.*

These functions are known by many different names including *Spherical Harmonics*, *surface harmonics* and the *Laplace Functions*. For purposes of our immediate discussion we will restrict ourselves to the Legendre Polynomials where $m = 0$. The first few of these functions are

$$\begin{aligned}
&P_0(\mu) = 1, && P_0(\theta) = 1\\
&P_1(\mu) = \mu, && P_1(\theta) = \cos\theta\\
&P_2(\mu) = \tfrac{1}{2}(3\mu^2 - 1), && P_2(\theta) = \tfrac{1}{4}(3\cdot\cos 2\theta + 1)\\
&P_3(\mu) = \tfrac{1}{2}(5\mu^3 - 3\mu), && P_3(\theta) = \tfrac{1}{8}(5\cdot\cos 3\theta + 3\cdot\cos\theta)
\end{aligned} \tag{3.4.36}$$

Fig. 3-3 shows a plot of the Legendre Polynomials in the polar coordinate θ. They represent a monopole ($n = 0$) a dipole ($n = 1$) and higher order quadrapoles ($n > 1$).

The Legendre Polynomials are an orthogonal set with

$$\int_{-1}^{1} P_n(\mu)\cdot P_m(\mu)\,d\mu = \begin{cases} 0 & n \neq m \\ \dfrac{2}{2m+1} & n = m \end{cases} \tag{3.4.37}$$

Now that we have complete solutions for the individual coordinates in the spherical case, we can write the general solution as

$$p(k,r,\theta) = \sum_n A_n P_n(\cos\theta) h_n(kr) \tag{3.4.38}$$

where we have, as usual, dropped the time exponential.

3.5 A Spherical Example[8]

The classic example problem in Spherical Coordinates is radiation from a polar cap. This is a good approximation to a loudspeaker in a box in free space even though it is not exactly correct. We will see later how to make this problem more realistic.

8. see Morse, *Vibration and Sound* or *Theoretical Acoustics*

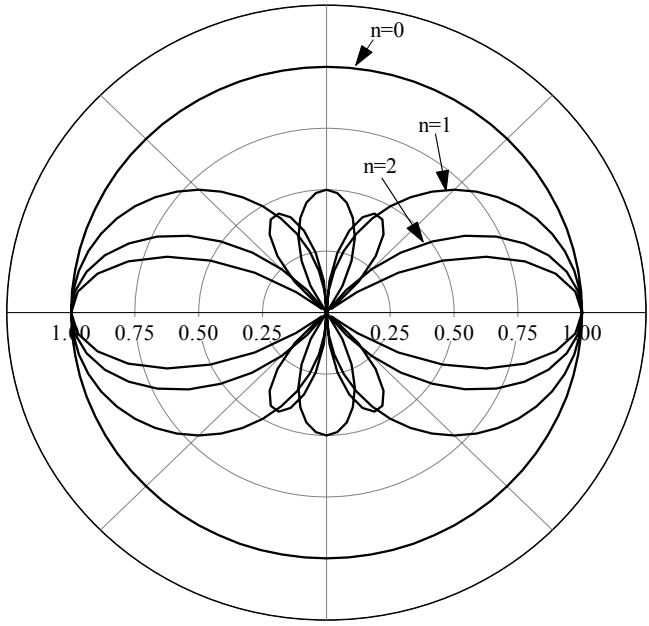

Figure 3-3 - Polar pattern for the angular modes of order n

The boundary condition for this problem is that at the radius of the sphere, a, we must have a given velocity v_0 over a section of the sphere given by $|\theta| < 30°$, a spherical cap. Thus we have

$$V(\theta) = \begin{cases} v_0 & -30° \le \theta \le 30° \\ 0 & otherwise \end{cases} \tag{3.5.39}$$

We first assume a solution as a finite series of solutions of the type shown in Eq. (3.4.38), and then apply the boundary conditions to obtain our solution. We must consider all possible solutions consistent with the separation constants. This will then determine the values for the unknown coefficients that fit the given boundary conditions. Proceeding, let the pressure field be

$$p(r,\theta) = \sum_n A_n P_n(\cos\theta)\, h_n(kr) \tag{3.5.40}$$

The boundary conditions can now be enforced by noting that

$$V(\theta) = \frac{1}{-ik\rho c} \frac{\partial p(kr,\theta)}{\partial r}\bigg|_{r=a} \tag{3.5.41}$$

(recall Eq. (3.1.6)) which results in

$$\sum_n A_n P_n(\cos\theta) h_n'(ka) = -i\rho c V(\theta) \tag{3.5.42}$$

Next we us the power of orthogonality by multiplying both sides of this equation by $P_n(\mu)$ and integrating from –1 to 1

$$-i\rho c \int_{-1}^{1} V(\theta) P_m(\mu) d\mu = \sum_n A_n \int_{-1}^{1} P_m(\mu) P_n(\mu) d\mu \, h_n'(ka) \tag{3.5.43}$$

Since the Legendre Polynomials are orthogonal we obtain (using Eq. (3.4.37), the orthogonality relationships for these polynomials)

$$-i\rho c \int_{-1}^{1} V(\theta) P_n(\mu) d\mu = A_n \frac{2}{2n+1} \; h_n'(ka) \tag{3.5.44}$$

and finally

$$A_n = -i\rho c \frac{(n+\frac{1}{2})}{h_n'(ka)} \int_{-1}^{1} V(\theta) P_n(\mu) d\mu \tag{3.5.45}$$

$$= -i\rho c \frac{(n+\frac{1}{2}) \cdot v_0}{h_n'(ka)} \int_{\cos 30°}^{1} P_n(\mu) \; d\mu$$

$$= -i\rho c \frac{v_0 \cdot \left(P_{n-1}(.87) - P_{n+1}(.87)\right)}{2 \cdot h_n'(ka)}$$

We can now insert these values for A_n back into Eq. (3.5.40) to get the final result

$$p(r,\theta) = \frac{i\rho c v_0}{2} \sum_n \frac{h_n(kr)}{h_n'(ka)} \left(P_{n-1}(.87) - P_{n+1}(.87)\right) P_n(\cos\theta) \tag{3.5.46}$$

Fig. 3-4 shows the polar response for various values of ka. (This plot is normalized to the axial response.) As the frequency goes up (increasing ka) the polar response narrows until a value of about $ka = 6$, at which point it begins to take on a pattern which has a more consistent directional response. This is the principle behind the concept of Constant Directivity (CD) – which says that at sufficiently high frequencies the sound radiates directly from the sources velocity profile, i.e. the angular variation of the radiated sound is the same as the velocity distribution on the sphere. This is asymptotically true at high frequencies, but the next figure shows that this is not really true for more practical frequencies where the wavelengths are not infinitesimally small. The frequency must be fairly high for the polar response to even begin to approach CD at the angle of the wavefront.

Shown in Fig. 3-5 is the same data as that shown in the figure above only in a different format. We will use this new format almost exclusively in later chapters, which is why we have introduced it. It is not the common format for presenting

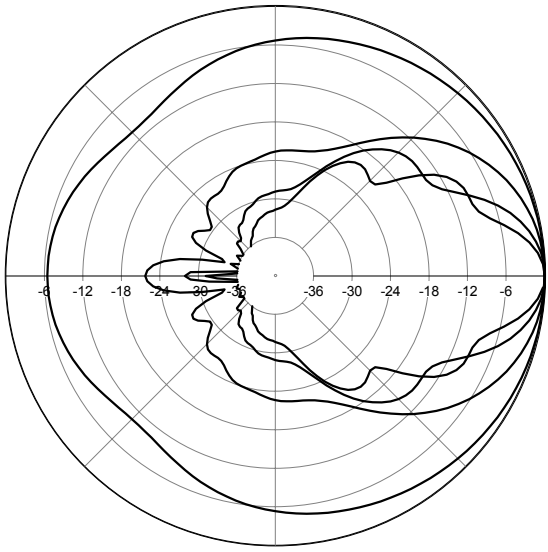

Figure 3-4 - Spherical radiation pattern for ka = 1,4,7&10

polar data, but this format is able to present the entire frequency variation of the polar response in one plane. The ka or frequency value is along the horizontal axis and the angle the vertical axis. The contours are usually at 6 dB intervals, although sometimes they are at 3 or 12 dB intervals. When the plot shows a transparent portion (the grid shows through, then the data is above the maximum level – usually 0 dB.

In this figure, we can more easily see CD occurring at about 30º, but not until we are substantially above $ka = 10.0$. Note that the directivity first narrows until about $ka = 10.0$, and then it begins to widen asymptotically approaching 30º at about -3 dB.

If we examine the pressure at the surface of the sphere $r = a$ in Eq. (3.5.46) we can see that the only terms in k (the frequency variable) are the Hankel Functions. If we divide Eq. (3.5.46) by an expression for the velocity we will obtain an equation containing only those terms which determine the frequency dependence of the radiation response. When normalized to ρc, these terms are called the modal impedances $z_m(ka)$

$$z_m(ka) = \frac{h_n(ka)}{h_n'(ka)} \,. \tag{3.5.47}$$

The modal impedances are shown in Fig. 3-6. These figures exhibit an important characteristic of sound radiation that we will find to be true of all radiation problems and that is mode cutoff. Note how each successive mode has a higher cutoff point below which it does not radiate sound to any appreciable degree.

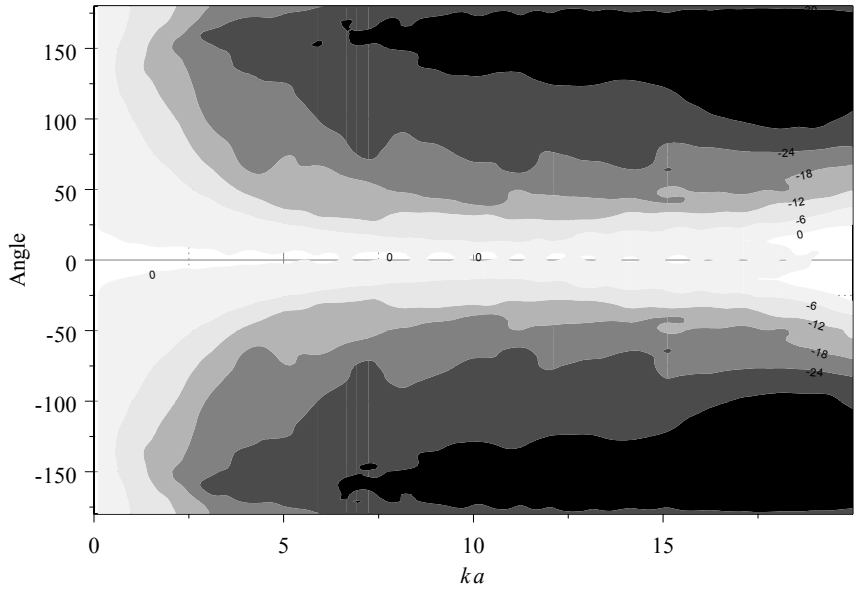

Figure 3-5 - Polar response plotted as a contour plot of ka value versus angle

Each impedance curve tends to peak at a ka value of $n+1$, where n is the order of the mode. The mass loading also increases with order but tends to peak at n. At low frequencies only the lowest order mode can contribute any of significant sound to the radiation. No matter how much we try to manipulate the velocity of the source, only that portion of the velocity that excites the lowest order mode will contribute to the sound radiation. We can see from this that at low frequencies, there is nothing that we can do to affect the polar radiation pattern, except null out the zero mode and utilize only higher order modes. But in so doing we must accept the extremely low radiation efficiency that will result. This characteristic is proof of something that we already knew to be true, but perhaps had never known exactly why.

Above about $ka = 1$, we can begin to affect the polar pattern to a limited degree. We will show a use for this effect in later chapters. These curves also show the degree to which the sound radiation diminishes at ever lower frequencies.

Finally, the modal radiation impedances are useful for calculating another important function. By simply integrating the angular terms over the surface of the spherical cap we can find a weighted sum of the modal impedance contributions to get the total radiation impedance for the source

$$z_{total}(ka) = \sum_n A_n \int_0^{30^\circ} \left(P_{n-1}(.87) - P_{n+1}(.87) \right) P_n(\cos\theta) \sin\theta \, d\theta \; z_n(ka) \qquad (3.5.48)$$

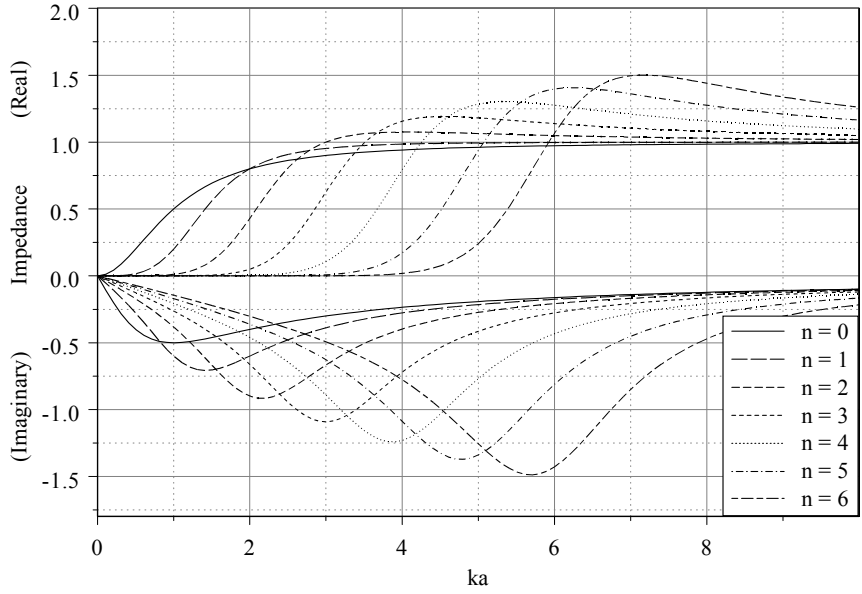

Figure 3-6 - Real and imaginary parts of the modal impedances for n= 0...6

The results of this calculation are shown below. When multiplied by the impedance of the medium ρc and divided by the area this impedance is the actual mechanical impedance seen by the diaphragm.

There is an interesting "trick" that can be performed with the spherical modal calculations. Since all odd modes have zero slope at $\mu = 0$ ($\theta = 90°$), by excluding all the even modes we can force a boundary condition of zero velocity in a plane through the sphere perpendicular to the axis of the source. In other words, the sphere is now a hemisphere placed against the wall. Fig.3-8 shows a comparison between the axial response for the free sphere and the hemisphere mounted against a wall. The wall reflections cause a fairly large variation in the response as they alternately add and subtract from the direct sound radiation due to phase delay effects. Fig.3-9 shows the polar map for this example. Comparing this map with the same portion of Fig.3-5 shows that placing the source against the wall has a lessor effect on the polar response except at low ka. The axial response is affected to a greater degree because the reflections are all in the same phase along this axis. If one must put a source against a wall, it is better to do so with the source at an angle to the wall than normal to it.

The impedance of this source could be calculated just as we did previously, but only considering the odd modes in the calculation. This exercise is left to the reader. By now the reader should also be able to describe the system (boundary conditions) that would result by taking only every fourth mode; or every sixth mode, etc. Another interesting exercise.

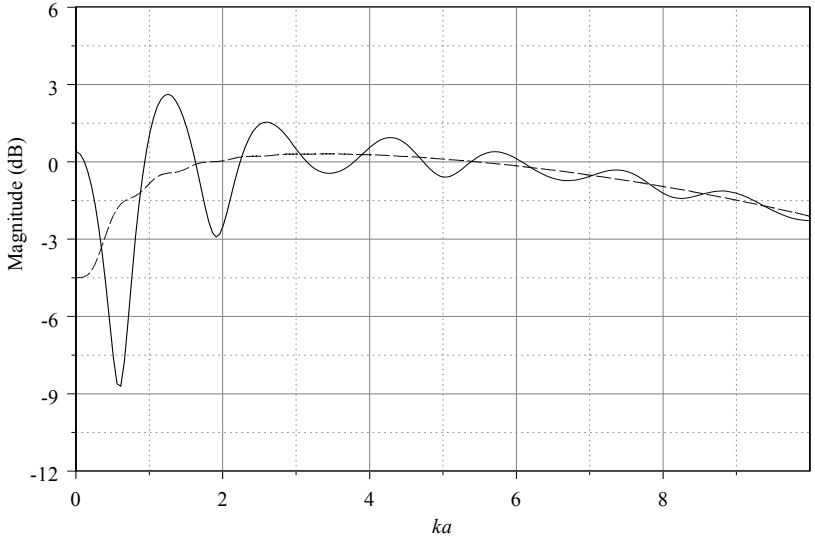

Figure 3-8 - Axial response comparison between free sphere and mounted sphere

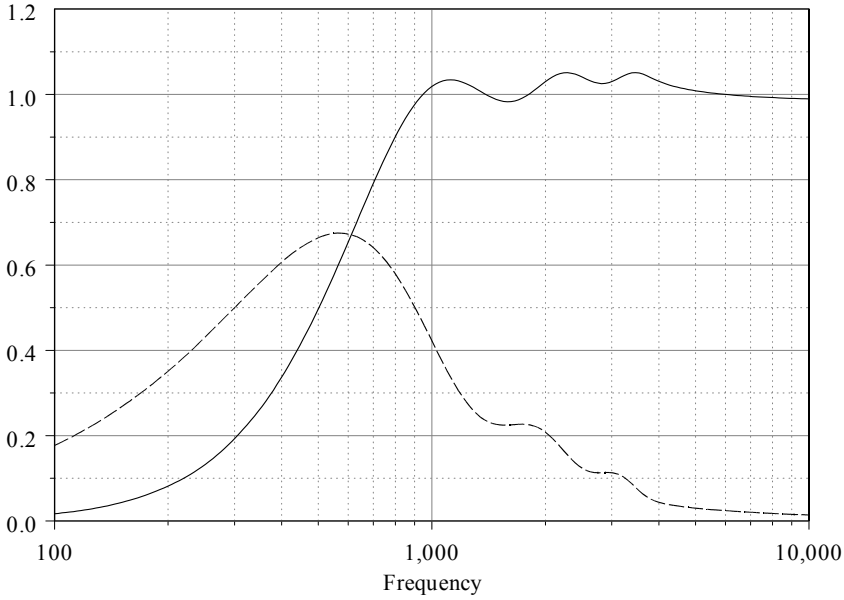

Figure 3-7 - Showing the calculated radiation impedance for a spherical cap

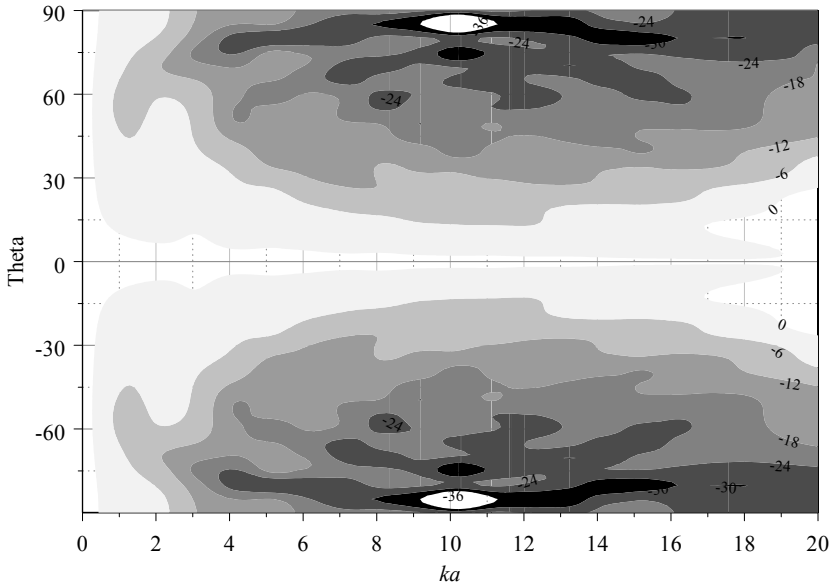

Figure 3-9 - Polar map for hemisphere against a wall

3.6 A Cylindrical Example

We will now show an example of sound radiation calculations in Cylindrical Coordinates. This will give us an opportunity to discuss a new technique for sound radiation problems. Consider the source shown in the figure below. This is an infinite cylinder with a source placed in its shell. The cylinder has a radius a and the source is defined as

$$V(\theta,z)=V_0\begin{cases}-30^0<\theta<30^0\\ |z|<b/2\end{cases} \qquad (3.6.49)$$

There are two ways to think about this problem, and to a first approximation the solutions are identical. First, we can think of this problem as a source placed on the shell of a cylinder such that it vibrates radially outwards. In reality it would be difficult to build such a source, at least not such that the velocity were uniform across the face. A

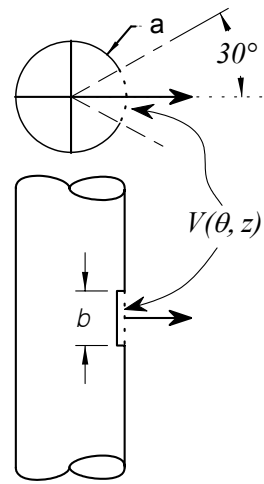

Figure 3-10 - Geometry for cylindrical radiation problem

bending source could be made to approximate this type of source, but it would likely have a diminished amplitude at the edges.

Another way to think about this source is to consider a line source at the center of the cylinder such that at the walls, where the hole or aperture is, the velocity is approximately uniform across the aperture. To a first order this is possible. To be exactly correct we would have to consider the effect of diffraction on the wavefront within the aperture and the effect that this diffraction would have on the velocity amplitude of the wave in the aperture. The diffraction in the aperture would act to alter the velocity distribution in the aperture so that it would not be uniform, as we have assumed. It turns out that this modification of the aperture velocity takes place principally in a frequency range where the wavelength is approximately the same as the aperture dimensions. Outside of this range this perturbation is negligible. Even in this range this effect is not a dominant one and ignoring it will only have a small (second order) effect on our results. We will take the approximate path and assume that the velocity is uniform in the aperture.

The problem shown above is of great interest to designers of the current genre of high performance sound reinforcement systems. These systems are being designed as large line arrays because of certain desirable features of these types of arrays. For the most part the theory of these systems is based on solutions for an infinite line array, not for a finite one. We will see that the two solutions are really quite different.

Since we have a know a solution for waves in the Cylindrical Coordinate system we can define the solution in terms of this set of these cylindrical waves. From previous sections, we know that the complete solution to an outgoing wave in this coordinate system is

$$p(r,\theta,z) = \sum_m \cos(m\theta) \int_{-\infty}^{\infty} B_m(k_z)\, H_m(k_r r)\, e^{i\, k_z z}\, dk_z \tag{3.6.50}$$

We have made two simplifications in this equation. First we have assumed that the source will be symmetric in θ and reduced the Fourier Series in θ to a single cosine function in m (no sine function), and second, the exponential term in k_z represents waves in both z directions so long as we don't restrict the sign of k_z. We must allow for all possible (symmetric) angular solutions and since the solutions in this coordinate are a discrete set in the integer m, this becomes an infinite sum. The solutions in the z direction have a separation constant k_z given by Eq. (3.6.51). The allowed values of k_z constitute a continuum in k-space and consequently the summation over all possible solutions in this coordinate becomes an integral in k_z. This integral is an example of the k-space formalism for sound radiation. The coefficients $B_m(k_z)$ consist of an indexed set of continuous functions which it is now our task to determine.

We have also excluded the second solution for the radial coordinate since we are interested only in waves that propagate outward from the source. We must also remember that kr is not completely arbitrary since

$$k = \frac{\omega}{c} = \sqrt{k_r^2 + k_z^z} \tag{3.6.51}$$

We are now in a position to apply the boundary conditions by setting Eq. (3.6.50) equal to the specified surface velocity

$$V(\theta, z) = \frac{1}{-ik\rho c} \frac{\partial p(r, \theta, z)}{\partial r}\bigg|_{r=a} \tag{3.6.52}$$

which results in

$$\sum_m \cos(m\ \theta) \int_{-\infty}^{\infty} B_m(k_z) k_r H_m^{'}(k_r a) \cdot e^{ik_z z} dk_z = -ik\rho c V_0 f(\theta) f(z) \tag{3.6.53}$$

where the prime on the radial function means that we must take its derivative with-respect-to (wrt) its argument (we must not forget to take the derivative of the argument wrt r which is where the kr comes from). The functions $f(\theta)$ and $f(z)$ are simply the angular and vertical velocity functions of Eq. (3.6.49), respectively.

Multiplying both sides of the above equation by $\cos(n\theta)\, e^{-ikzz}$ and then integrating over θ from $\theta = -\pi$ to π and $z = -\infty$ to ∞ will yield

$$\begin{aligned} &-ik\rho c V_0 \int_{-\pi}^{\pi} f(\theta)\cos(n\theta) d\theta \int_{-\infty}^{\infty} f(z) e^{-ik_z z} dz = \\ &\int_{-\pi}^{\pi} \sum_m \cos(m\theta)\cos(n\theta) d\theta \int_{-\infty}^{\infty} \int_{-\infty}^{\infty} k_r H_m^{'}(k_r a)\, B_m(k_z)\, e^{ik_z z} dk_z e^{-ik_z z} dz \end{aligned} \tag{3.6.54}$$

By the features of orthogonality (without which we are virtually helpless), and the Fourier Transform in k-space, which in this case simply returns the original function (the double integral is a transform and its inverse).

Eq. (3.6.54) simplifies to

$$-ik\rho c V_0 \int_{-\pi}^{\pi} f(\theta)\cos(n\theta) d\theta \int_{-\infty}^{\infty} f(z) e^{-ik_z z} dz = 2\pi B_m(k_z) k_r H_m^{'}(k_r a) \tag{3.6.55}$$

from which we can immediately determine the coefficients $B_m(k_z)$ as

$$B_m(k_z)\ = -i\rho c \frac{kV_0}{k_r H_m^{'}(k_r a)} A_m\, F(k_z) \tag{3.6.56}$$

where

$$A_m = \int_{-\pi}^{\pi} f(\theta)\cos(\theta) d\theta \tag{3.6.57}$$

and

$$F(k_z) = \frac{1}{2\pi} \int_{-\infty}^{\infty} f(z) e^{-ik_z z} dz \tag{3.6.58}$$

We should immediately recognize these as a Fourier Series for the discrete θ coefficients and a Fourier Transform for the continuous k_z coefficients. The last step in this calculation is to reinsert Eq. (3.6.56) into Eq. (3.6.50)

$$p(r,\theta,z) = -i\rho c k V_0 \sum_m A_m \cos(m\theta) \int_{-\infty}^{\infty} \frac{F(k_z) H_m(k_r r) \cdot e^{ik_z z}}{k_r H_m'(k_r a)} dk_z \tag{3.6.59}$$

Now using Eq. (3.6.51) we get the daunting equation

$$p(r,\theta,z) = -i\rho c k V_0 \sum_m A_m \cos(m\theta) \int_{-\infty}^{\infty} \frac{F(k_z) H_m\left(\sqrt{k^2 - k_z^2}\, r\right) e^{ik_z z}}{\sqrt{k^2 - k_z^2}\, H_m'\left(\sqrt{k^2 - k_z^2}\, a\right)} dk_z \tag{3.6.60}$$

Analytical solutions of this equation are not possible, but there are still ways that we can proceed. The most direct way is to use the approximate method of integration know as the method of stationary phase, which is similar to other approximate methods of integration (steepest decent, saddle point integration, etc.). This subject as a whole is beyond the scope of what we are interested here, but we will summarize the pertinent results.

The method of stationary phase states: for some complex integral $I(z)$

$$I(z) = \int_A^B f(z) e^{itg(z)} dz \cong (1+i) f(z_0) \quad e^{itg(z_0)} \sqrt{\frac{\pi}{tg''(z_0)}} \tag{3.6.61}$$

where

$$t \to \infty$$

$$g'(z_0) = 0$$

This method can be used on Eq. (3.6.60) if we consider only the far field, i.e. $R \to \infty$. In this case we must simplify the Hankel Function in the numerator in order to get a form on which to apply the method. If we let $z = R \sin\varphi$ with R large then

$$\begin{aligned} &\sqrt{\frac{2}{\pi r}} e^{-i(2m+1)\pi/4} \int_{-\infty}^{\infty} \frac{F(k_z)\ e^{-i\,R\sqrt{k^2-k_z^2}\cos\varphi}\ e^{i\,k_z R\sin\varphi}}{\left(k^2 - k_z^2\right)^{3/4} H_m'\left(\sqrt{k^2 - k_z^2}\, a\right)} dk_z \\ &= \sqrt{\frac{2}{\pi r}} e^{-i(2m+1)\pi/4} (1+i) f(z_0) \quad e^{itg(z_0)} \sqrt{\frac{\pi}{tg''(z_0)}} \end{aligned} \tag{3.6.62}$$

where we have used

$$t = R$$
$$g(k_z) = -(k^2 - k_x^2)\cos\varphi + k_z \sin\varphi$$
$$\varphi = vertical\ \ angle\ \ off\ \ axis$$

To find z_0 we set $g'(k_z) = 0$

$$\frac{d(-\sqrt{k^2 - k_x^2}\cos\varphi + k_z \sin\varphi)}{dk_z} = 0$$

to get

$$\sqrt{k^2 - k_x^2}\sin\varphi = k_z \cos\varphi$$
$$k_z = k\sin\varphi = z_0$$

Using this result in leads to

$$I(k) = \frac{F(k\sin\varphi)}{\left(k^2\cos^2\varphi\right)^{3/4} H_m^{'}\left(ka\sin\varphi\right)}\ e^{-ikR+\pi/4}\sqrt{\frac{\pi k\cos^2\varphi}{R}} = \sqrt{\frac{\pi}{R\cos\varphi}}\frac{F(k\sin\varphi)}{kH_m^{'}\left(ka\sin\varphi\right)}\ e^{-ikR+\pi/4} \tag{3.6.63}$$

which after some further simplifications yields

$$p(R,\theta,\varphi) = -i\sqrt{2}\rho c V_0 \frac{e^{-ikR}}{kR\cos\varphi}\sum_m A_m e^{-im\pi/2}\cos(m\theta)\ \frac{F(k\sin\varphi)}{H_m^{'}\left(ka\sin\varphi\right)} \tag{3.6.64}$$

This equation is only valid for large R. It has been shown that this result becomes exact as $R \to \infty$.

We are now in a position to find the values of the coefficients and look at some results. The θ coefficients are easily determined

$$A_m = 2\int_0^{\pi/6}\cos(m\theta)d\theta = \frac{\sin\left(m\pi/6\right)}{m} \tag{3.6.65}$$

The $F(k\sin\varphi)$ coefficients are likewise straightforward to calculate since the Fourier Transform of the $\mathrm{Rect}(kb\sin\varphi/2)$ function is well known

$$F(k\sin\varphi) = \mathrm{Rect}\left(\frac{kb\sin\varphi}{2}\right) = \frac{1}{2\pi}\int_{-b/2}^{b/2} f(z)e^{-ik\sin\varphi z}dz = \frac{b}{2\pi}\frac{\sin(kb\sin\varphi)}{kb\sin\varphi} \tag{3.6.66}$$

Finally the far field solution can be written as

$$p(r,\theta,\varphi) = -i\rho c b V_0 \frac{e^{ikR}}{kR} \frac{\sin(kb\sin(\varphi))}{kb\sin(\varphi)} \cdot \sum_m \frac{\sin(m\pi/6)}{m} \frac{i^m}{\cos(\varphi)\ H_m'(ka\cos(\varphi))} \cos(m\ \theta) \tag{3.6.67}$$

Fig. 3-11 shows the polar pattern in the horizontal plane. The cylinder in this example is about two feet across (r=.3 m) and the source about eight inches across (20 cm). The source is continuous about one meter in total height. The plots are normalized to the axial response which we will look at in more detail later. In this figure the modal calculations are not likely to have sufficient content

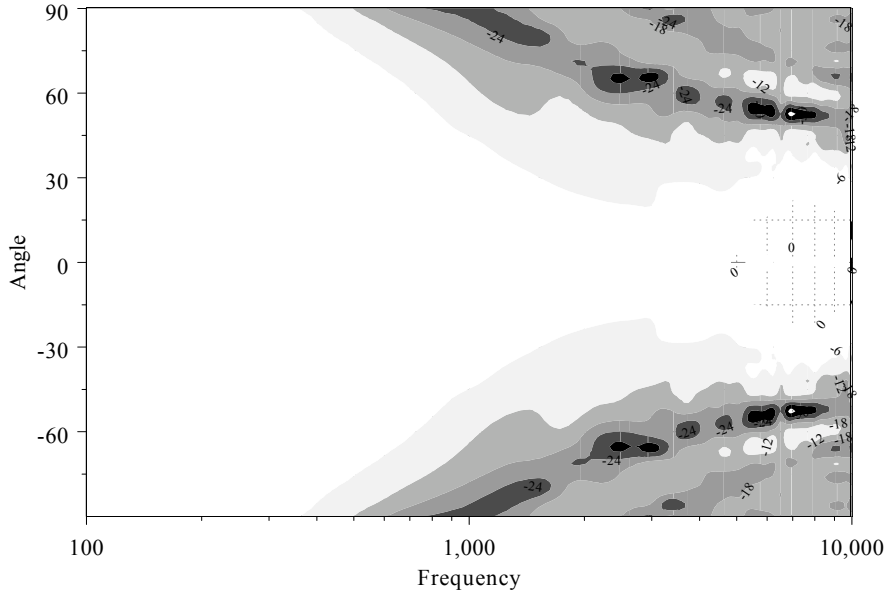

Figure 3-11 - Horizontal polar response for a line source on a cylinder

after about 5 kHz so the results in the higher frequencies may not be correct. There were 40 modes in this calculation and the Hankel Functions for small argument, which go to infinity, tend to get unstable at higher mode numbers. Note that the horizontal response narrows to around ±30° remaining almost constant at about -6 dB.

Fig. 3-12 shows the polar response in the vertical plane. Almost all of the energy is directed towards the central axis. We have plotted only to 60° since the results for larger angles fluctuate so rapidly that the plotting algorithm fails. Note that at higher frequencies the results are suffering from an instability in either the numerical calculations of the function or the contour plotting routine (which uses

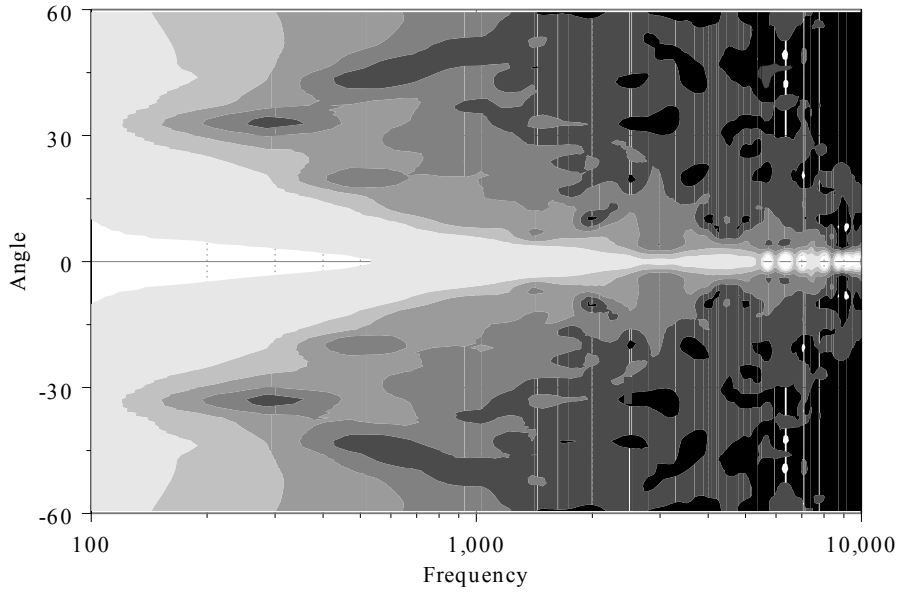

Figure 3-12 - Vertical polar pattern for cylindrical radiator

interpolative smoothing) or both. The interesting thing to note here is that we might expect this same effect in an actual device, namely that the response has become hypersensitive to small variations and exhibits an unstable condition like that shown in the plot. In a real situation the vertical polar response in this regime could fluctuate with small variations in temperature, air currents, atmospheric pressure or humidity. Unlike light, the acoustic wave speed can change by relatively large percentages in short distances. This can cause a sort of acoustic shimmering similar to the twinkling that we see when we look at the stars, only this effect occurs on a much smaller scale of wave travel. We will see these same phenomena when we talk about room acoustics in Chap. 7.

Finally Fig. 3-13 shows the response of this array on axis for a constant acceleration array of drivers. The apparent constant directivity does not come without a cost – namely a continuously falling axial response. This response falloff must be recovered with some form of gain, but 40 dB is a lot of loss to make up.

A calculation of the modal radiation impedances can be obtained from the previous example by setting the argument of Hankel Function in the numerator of Eq. (3.6.60) equal to ka, and performing the integrations via other simplifications. However this would not be constructive in the general case since these impedances would depend on the vertical arraignment of the source. An easy calculation is to calculate the modal impedance z for a uniform vertical velocity on the cylinder. In this case, the function $F(k_z)$ would become $\delta(0)$ and the integra-

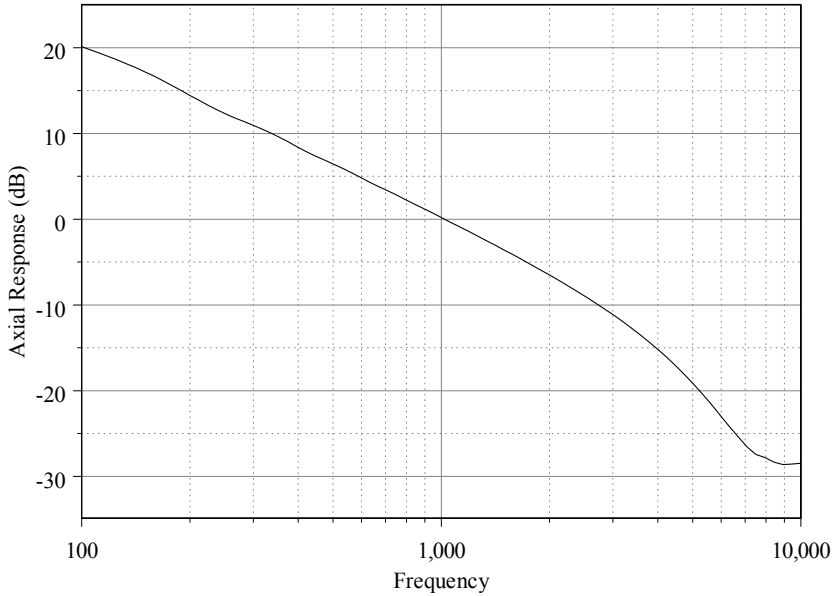

Figure 3-13 - Axial frequency response for cylindrical radiator

tion would be trivial. The modal impedances for this simplified example are shown in Fig.3-14 for the real and imaginary parts respectively of the first six modes.

3.7 The Cylindrical Near Field

The characteristic of the above line source in the near field are very important owing to the fact that the near field extends a considerable distance into the sound field for this type of source. The solution of Eq.(3.6.64) cannot be directly analyzed for the near field, but we can use another method.

At this point we need to introduce another technique for sound field calculations that are based on the Green's Function. The Green's Function is the spatial analog to the impulse response in systems theory. Once we know the pressure at the observation point r (the output response), due to a point source at point r_0 (a spatial impulse), the result for any source distribution is simply the integral over all of the point sources that make up the desired source. This result is exactly analogous to calculating the output of a system for an arbitrary input by using the systems impulse response. This technique is very powerful, so long as the Green's Function is known (which is usually the difficult part). We will use such an approach here.

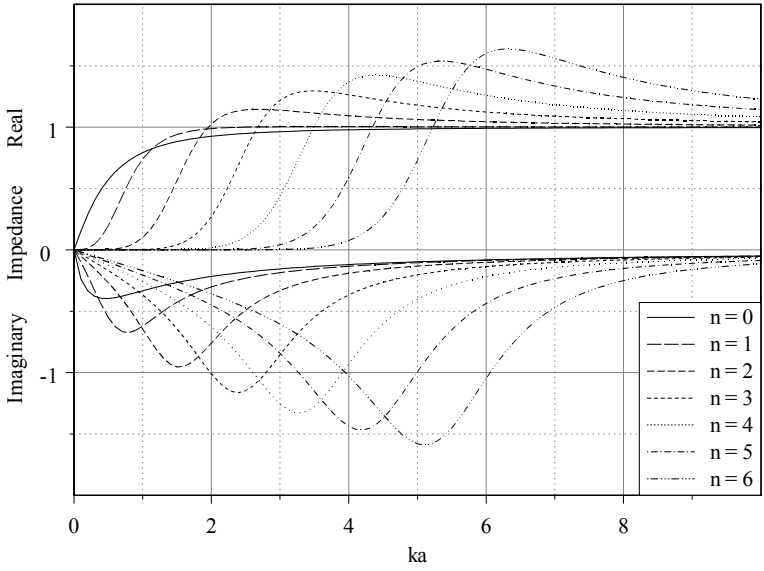

Figure 3-14 - Modal radiation impedances for cylindrical radiator

The Green's Functions in infinite space (boundary at ∞) are

Dimensions	Green's Function $g(x\|x_0)$
1	$\frac{2\pi i}{k} e^{ik\|x-x_0\|}$
2	$i\pi H_0\left(k\,\|\,r-r_0\,\|\right)$
3	$\frac{e^{ik\|r-r_0\|}}{\|\,r-r_0\,\|}$

Table 3.1: Green's Functions

Those for the single and three dimensional spaces are quite simple, while the two dimensional one is not so simple. Solutions of radiation problems involving boundaries which are not separable, and hence not analytically solvable, can be obtained by using the three dimensional Green's Function along with Green's Theorem to yield an integral equation over the surface of the radiating object. This technique can be applied to any shape boundary and is sometimes referred

to as the Boundary Integral Method (BIM). (Although in general the Boundary Integral Method is more general than applying to sound radiation problems.) These techniques are also very powerful, and the interested reader is encouraged to investigate them. They will not be discussed in this text because doing so would take us far away from our intent, which is a thorough overview of the fundamental physics of transducers. Like the FEM, which we discussed in Chap. 2, the BIM is best applied to specific cases where in depth analysis is warranted by application. BIM solutions are specific to the particular analysis being performed and generalizations of results are difficult to impossible to obtain, unlike the modal solutions that we have been studying here.

Looking now at our particular problem we want to use the two dimensional Green's Function to look at the near field of our radiating cylinder. When the source is independent of the axial coordinate z then a simple integral results

$$p(r,\theta) = i\rho ck \int_{-\theta_0}^{\theta_0} v_0(\theta) g_k(|\, r - r_0\,|) d\theta \tag{3.7.68}$$

where the Green's Function must be one that satisfies the boundary conditions on the cylinder. This can be accomplished by using an expansion of the Hankel Function and adding a second expansion which represents the reflection from the rigid boundary. This equation then has its gradient set equal to zero at the surface of the cylinder. We would eventually end up with exactly the same equations that we obtained from the modal expansion result for this case.

On the other hand when we place ourselves in a plane of symmetry (the *r-z* plane) then the boundary condition for the Green's Function is simply twice the free space Green's Function when r_0 is on the surface and $r > r_0$. There is one more complication to this problem and that is that the space into which the source is radiating is expanding, i.e. increasing with *r* at the rate of $1/\sqrt{r}$. We can still use the Green's Function approach so long as we recognize that the two dimension axi-symmetric problem must have an additional $1/\sqrt{r}$ term in it to account for this coordinate expansion. This extra factor is obvious by considering that the far-field for any finite source must fall as $1/r$ for large *r*. This is true in any coordinate system. The Hankel Function for large argument only falls as $1/\sqrt{r}$.

Using the two dimensional Green's Function, the equation for radiation in the *r-z* plane from an axi-symmetric source which is finite in *z* then becomes

$$p(R,\varphi) = i\rho ck \int_{-b}^{b} v_0(z_0) \frac{H_0(kR(z_0)\sin\varphi)}{R(z_0)\cos\varphi} dz_0 \tag{3.7.69}$$

$$R(z_0) = \sqrt{r^2 - 2r z_0 \sin\varphi + z_0^2}$$

with the variables as shown in Fig. 3-15.

While this is not exactly the calculation that we wanted to do (it has a source that circumnavigates the cylinder) it will give us a good indication of the near field

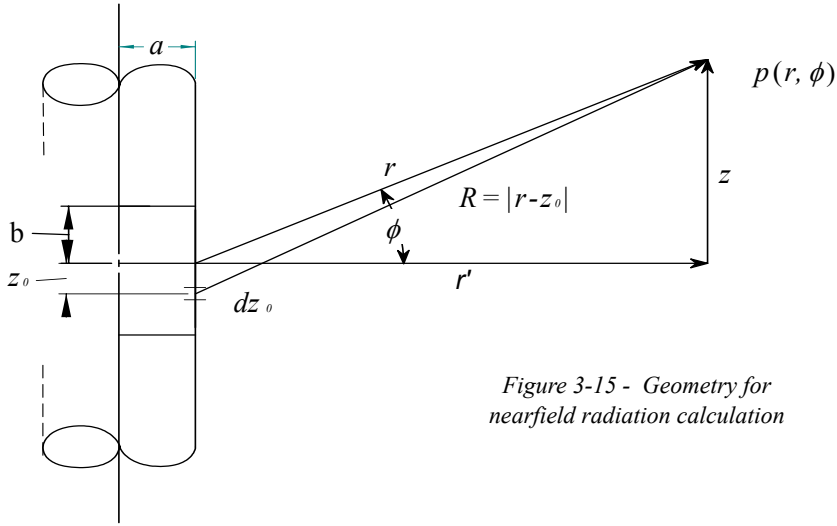

Figure 3-15 - Geometry for nearfield radiation calculation

effect for the higher frequencies where the radiation from the rear of the cylinder to the front becomes negligible. The results therefore become correct as the frequency increases.

Eq. (3.7.69) is easily calculated numerically. The calculation of the sound field on axis as a function of distance from the source is shown in Fig. 3-16 The solid lines at the bottom of the graph show the -6 and -12 dB/octave slopes indicating that the field falls off initially at -6 dB/octave, but changes to -12 dB/octave at a distance from the source that moves out with higher frequency. The region where the falloff is slower is know as the near field. The near field extends out to approximately

$$r = .11 \cdot k a \text{ m.}$$

a = *height of the line array*

We can also see that within the near field the frequency response is highly irregular.

Another way of viewing the near field is shown in Fig. 3-17. This figure shows the response for a constant velocity source (not the usual situation; usually the source velocity falls and so this response would fall like that shown in the figure below). Here we can see that the frequency response for the cylindrical source is changing with the distance from the source in a highly complex manner.

There is no hope of equalizing this response to flat at all locations. Generally speaking this characteristic – changing frequency response with distance - is true of the near field of any source. It is for this reason that the near field is not usually a good place for a listener.

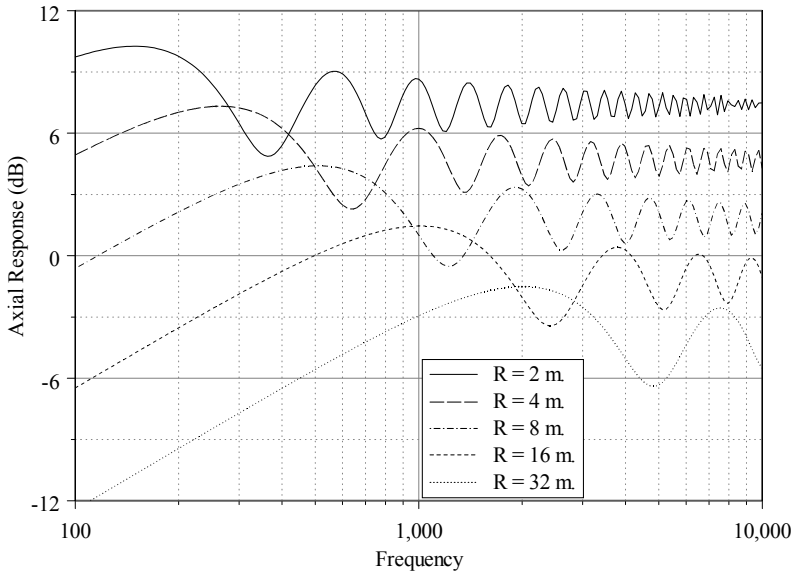

Figure 3-17 - Axial frequency response at various distances from the source

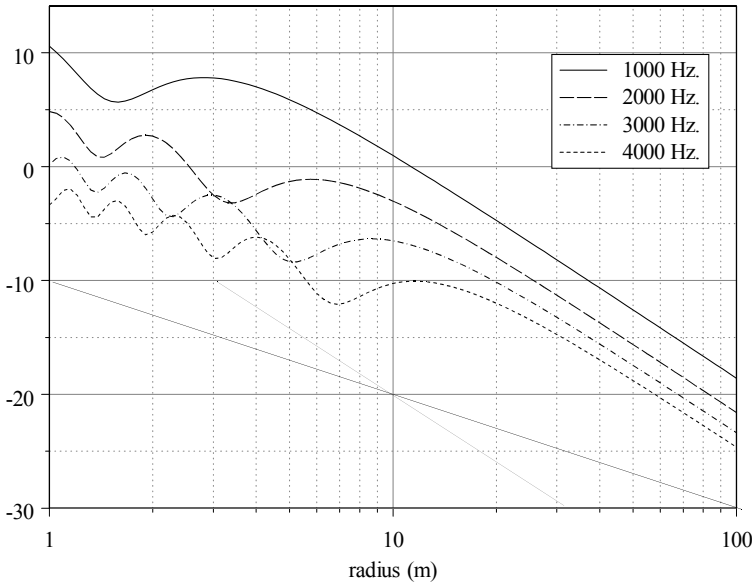

Figure 3-16 - Nearfield axial pressure for a line array

3.8 Summary

This chapter has shown the basic acoustical equations for sound radiation in a few coordinate systems. Several examples were shown which typify the radiation characteristics of audio frequency transducers. In the next several chapters, we will look at more specialized sound radiators and introduce some new techniques for handling calculations in an efficient manner. Almost invariably these techniques will rely on the modal description of the sound field that we have studied in this chapter.